Antiviral Research 158 (2018) 113–121

Contents lists available at ScienceDirect

Antiviral Research

journal homepage: www.elsevier.com/locate/antiviral

Alkyl-imino sugars inhibit the pro-oncogenic ion channel function of human papillomavirus (HPV) E5

Laura F. Wetherill[a,c,d,1], Christopher W. Wasson[a,d,1], Gemma Swinscoe[a,d], David Kealy[a,d], Richard Foster[b,d], Stephen Griffin[c,d,2], Andrew Macdonald[a,d,*,2]

[a] School of Molecular and Cellular Biology, Faculty of Biological Sciences, UK
[b] School of Chemistry, Faculty of Mathematics and Physical Sciences, University of Leeds, Leeds, LS2 9JT, UK
[c] School of Medicine, Faculty of Medicine & Health, University of Leeds, Wellcome Trust Brenner Building, St James' University Hospital, Beckett St., Leeds, LS9 7TF, UK
[d] Astbury Centre for Structural Molecular Biology, University of Leeds, Leeds, LS2 9JT, UK

ARTICLE INFO

Keywords:
HPV
Viroporin
EGFR signalling

ABSTRACT

Despite the availability of prophylactic vaccines the burden of human papillomavirus (HPV) associated malignancy remains high and there is a need to develop additional therapeutic strategies to complement vaccination. We have previously shown that the poorly characterised E5 oncoprotein forms a virus-coded ion channel or viroporin that was sensitive to the amantadine derivative rimantadine. We now demonstrate that alkylated imino sugars, which have antiviral activity against a number of viruses, inhibit E5 channel activity *in vitro*. Using molecular modelling we predict that imino sugars intercalate between E5 protomers to prevent channel oligomerisation. We explored the ability of these viroporin inhibitors to block E5-mediated activation of mitogenic signalling in keratinocytes. Treatment with either rimantadine or imino sugars prevented ERK-MAPK phosphorylation and reduced cyclin B1 expression in cells expressing E5 from a number of high-risk HPV types. Moreover, viroporin inhibitors also reduced ERK-MAPK activation and cyclin B1 expression in differentiating primary human keratinocytes containing high-risk HPV18. These observations provide evidence of a key role for E5 viroporin function during the HPV life cycle. Viroporin inhibitors could be utilised for stratified treatment of HPV associated tumours prior to virus integration, or as true antiviral therapies to eliminate virus prior to malignant transformation.

1. Introduction

Human papillomaviruses (HPV) are small non-enveloped double-stranded DNA (dsDNA) viruses that infect squamous epithelial cells. They are sexually transmitted causing approximately 5 million new infections per year in the USA (Cates, 1999). Mucosal, low-risk HPV types cause benign anogenital warts, whereas a limited number of high-risk HPV types cause the majority of anogenital cancers as well as a subset of oropharyngeal malignancies; HPV16 and HPV18 are responsible for the largest proportion of carcinomas (de Sanjose et al., 2010; Prigge et al., 2017; Walboomers et al., 1999). Prophylactic vaccines are available, yet these protect against only a sub-set of HPV types with little impact upon pre-existing infections (Schiller and Müller, 2015). Moreover, HPV vaccination programmes are poorly available in most developing countries where cervical cancer is more frequent (Bruni et al., 2016). Effective antiviral agents represent an alternative approach to treating HPV infections, yet no such drugs are currently available.

High-risk HPV encodes three early oncogenes (E5, E6 and E7) that influence cellular proliferation, differentiation and survival (Moody and Laimins, 2010). E6 and E7 functions are well characterised as the major drivers of keratinocyte proliferation, and their expression is retained within tumours.

By contrast, E5 is less well understood. High-risk E5 expression induces anchorage-independent growth in murine fibroblasts and growth in low serum, as well as transformation of primary human keratinocytes (Müller et al., 2015a). Mice transgenic for epithelial HPV16 E5 expression display hyperplasia and spontaneous tumour formation (Maufort et al., 2007), with increased cervical dysplasia (Maufort et al., 2010a). E5 mRNA is highly abundant in HPV lesions (Stoler et al.,

* Corresponding author. Faculty of Biological Sciences, University of Leeds, Leeds, West Yorkshire, LS2 9JT, UK.
E-mail address: a.macdonald@leeds.ac (A. Macdonald).
[1] These authors contributed jointly to the manuscript.
[2] Joint corresponding authors.

https://doi.org/10.1016/j.antiviral.2018.08.005
Received 10 March 2018; Received in revised form 27 July 2018; Accepted 6 August 2018
Available online 07 August 2018

1992), and the protein is likely expressed in the early stages of malignancy, when episomal viral genomes are present (Chang et al., 2001). Thus, E5 represents a potential target for early stage intervention in HPV positive cancers.

E5 potentiates epidermal growth factor receptor (EGFR) signalling, resulting in enhanced mitogen activated protein kinase (MAPK) activity (Straight et al., 1993; Wasson et al., 2017). E5 modulation of EGFR is implicated in pathogenesis, and expression of a dominant negative EGFR attenuates epithelial hyperplasia observed in E5-transgenic mice (Genther Williams et al., 2005). The generation of high-risk HPV genomes lacking E5 expression has identified a key role during the productive stages of infection (Fehrmann et al., 2003; Genther et al., 2003; Wasson et al., 2017). Recently, EGFR activation has been shown to be critical for E5 function during the productive stages of the HPV lifecycle (Wasson et al., 2017). In the absence of EGFR signalling, HPV18 containing keratinocytes fail to maintain cyclin B1 expression in the suprabasal layers of the epithelium and instead initiate default differentiation programmes. Precisely how EGFR signalling is augmented by E5 is unknown, but may involve E5-mediated alkalinisation of EGFR-containing endosomes, preventing degradation, and resulting in recycling of activated receptor to the plasma membrane (Straight et al., 1995). How E5 perturbs endosome acidification remains unknown.

E5 belongs to an expanding group of viral membrane proteins termed viroporins (Royle et al., 2015; Scott and Griffin, 2015). These small proteins (50–120 residues) contain at least one pore-forming helix, which oligomerises to create a hydrophilic pore across membranes. Viroporins perturb host cell homeostasis at various stages during infection, often involving viral entry and/or release (Scott and Griffin, 2015). However, other cellular functions can also be altered by these proteins, including vesicle trafficking and apoptosis. Inhibition of viroporin function represents an ideal target for antiviral drug development (Scott and Griffin, 2015), with clinical precedent set by prototypic adamantane drugs targeting the influenza A virus (IAV) M2 proton channel (Pinto et al., 1992).

We previously demonstrated that HPV16 E5 forms a hexameric viroporin complex, with activity sensitive to the adamantane rimantadine, as well as novel unrelated scaffolds (Wetherill et al., 2012). Here, we now identify alkyl imino sugars as inhibitors of E5 viroporin activity. Ensuing blockade of channel activity prevents E5-mediated activation of ERK-MAPK resulting in diminished cyclin B1 expression within suprabasal keratinocytes and concomitant block to the HPV18 life cycle. Thus, targeting E5 channel activity represents a viable drug target with potential for both antiviral and anti-tumour applications.

2. Methods and materials

2.1. Recombinant E5 protein expression and purification

FLAG-E5 was expressed as a glutathione *S*-transferase (GST) fusion in *Escherichia coli* cells and then cleaved and purified as described previously (Wetherill et al., 2012).

2.2. Liposome permeability assays

Rhodamine-labelled liposomes comprised of phosphatidic acid and phosphatidylcholine containing self-quenching concentrations of carboxyfluorescein (CF) were generated as described (Wetherill et al., 2012). FLAG-E5 induced CF release was assessed by real-time fluorimetry (FLUOstar Optima microplate reader, BMG Technologies). Excitation and emission filters set to 485 and 520 nm, respectively) in reactions typically comprising 1 μg protein and 50 μM liposomes in a total reaction volume of 100 μl with HBS, giving a final E5 concentration of ~1 μM, as described (Wetherill et al., 2012). 1 μM melittin (Sigma) served as a positive control. All samples were repeated in triplicate, and data were averaged. Endpoint readings were taken or initial rates were calculated from the initial linear dye release kinetics ($\Delta FU\ s^{-1}$), where FU are fluorescence units.

2.3. E5 inhibitor compounds

Compounds used were rimantadine-HCl (Sigma), hexamethylene amiloride (HMA) (Sigma), and the imino sugar derivatives *N*-nonyl deoxynojirimycin (*NN*-DNJ) and *N*-nonyldeoxygalactonojirimycin (*N*B-DGJ) (Toronto Biochemicals). All inhibitors were reconstituted as 40 mM stock solutions in DMSO, then diluted as appropriate in media or buffer.

2.4. In silico modelling of E5 and binding studies

The secondary structure of E5 was predicted by using PSIPRED (http://bioinf.cs.ucl.ac.uk/psipred) and MEMSAT3. Models of the E5 monomer were constructed by using Maestro (Schrodinger Inc.) as previously described (Wetherill et al., 2012). Monomers were built amino acid by amino acid with energy minimization (Merck molecular force field [MM/FF] in a simulated water dielectric). Monomers were docked into an oligomer and subjected to further energy minimization. Docking against E5 complexes employed the LigPrep module of Maestro in the Schrodinger docking program Glide (Friesner et al., 2004). The LigPrep-treated and energy-minimized ligand was docked into the prepared receptor grid, and the binding affinity was evaluated with the Glide score (GScore) parameter (Eldridge et al., 1997). The best-docked pose was selected as the one with the lowest GScore, the highest negative value.

2.5. Cell culture

C33A cells were maintained as described previously (Müller et al., 2015b). Transfection of primary human foreskin keratinocytes (NHK) isolated from neonate foreskin tissues (ethical approval no. 06/Q1702/45) was performed as described previously (Delury et al., 2013; Wilson et al., 2005). To account for donor-specific effects, cell lines harbouring wild type or E5 knockout (E5KO) HPV18 genomes were generated in NHK isolated from two donors.

2.6. High calcium differentiation assay

HPV18 containing NHK were grown in complete E media until 90% confluent. Media was changed to serum free keratinocyte media without supplements (SFM medium, Invitrogen) containing 1.8 mM calcium chloride. Cells were maintained in this media for between 48 and 72 h before lysis and analysis.

2.7. Western blotting

Total protein was extracted from keratinocytes in lysis buffer (Mankouri et al., 2010) and resolved by SDS-PAGE (10–15% Tris-Glycine), transferred onto Hybond nitrocellulose membrane (Amersham biosciences) and probed with antibodies specific for cyclin B1 (H-433, Santa Cruz Biotechnology), HPV18 E6 (G-7, Santa Cruz Biotechnology), HPV18 E7 (8E2, Abcam (ab100953), phospho-ERK1/2 (43705, Cell Signalling Technology), GFP (sc-9996, Santa Cruz Biotechnology) and GAPDH (G-9, Santa Cruz Biotechnology). Immunoblots were visualized with species-specific HRP conjugated secondary antibodies (Sigma) and ECL reagent (Thermo/Pierce).

2.8. Cytotoxicity assays

Cells were plated in 96-well plates 24 h prior to treatment with E5 inhibitors. Cell viability was determined 24 h post-treatment by MTT assay as described previously (Samson et al., 2016).

2.9. Measurement of cell membrane lipid packing

Membrane lipid packing was studied using the fluorescent probe, MC540 (Sigma), assessing the degree of membrane insertion by fluorescence flow cytometry (Suzuki et al., 2010; Williamson et al., 1983). GFP or GFP18E5 transfected C33A cells were incubated for 48 h, then detached using an enzyme-free/PBS-based cell dissociation buffer. Cells were suspended in 10 µg/ml MC540/PBS for 10 min at 37 °C, then washed thoroughly in PBS before resuspension in 250 µl PBS. Cell surface fluorescence was analysed with a BD Fortessa used at 488 nm excitation and 575 nm emission wavelengths.

2.10. Luciferase reporter assay

C33A cells were transfected by using polyethyleneimine (PEI) reagent as described in (Müller et al., 2015b) with plasmids expressing GFP and GFP-18E5 in combination with a reporter plasmid in which the human cyclin B1 (CCNB1) promoter drives the expression of firefly luciferase (Wasner et al., 2003). A constitutively expressing *Renilla* luciferase plasmid was used to assess transfection efficiency. Transfected cells were serum starved for 12 h and then lysed and assayed for luciferase activities by using Dual-Luciferase Stop and Glo reagent (Promega) and a luminometer (EG&G Berthold) as described (Richards et al., 2015). Where appropriate, cells were treated with rimantadine or *N*N-DNJ (10 µM) for 12 h prior to analysis. All assays were performed in triplicate. Fold promoter activity was calculated by dividing the relative luciferase activity of stimulated cells by that of mock-treated cells.

3. Results

3.1. Inhibition of E5 channels by imino sugar derivatives

Several prototypic classes of inhibitor compounds have been shown to abrogate viroporin function *in vitro* including rimantadine, nonylated imino sugars (e.g. *N*N-DNJ) and hexamethylene amiloride (HMA) (Scott and Griffin, 2015). These compounds have since been shown to exert antiviral effects against a number of viruses including HCV, BVDV, Dengue and SARS-CoV (Pavlović et al., 2003; Stgelais et al., 2009; Wilson et al., 2006; Wu et al., 2002; Zitzmann et al., 1999). As rimantadine effectively blocks HPV16 E5 activity (Wetherill et al., 2012), we examined whether other prototypic viroporin inhibitors might block 16E5 viroporin activity in an *in vitro* liposome dye release assay (Fig. 1A) (Wetherill et al., 2012), namely HMA, the long alkyl-chain imino sugar *N*N-DNJ and the short alkyl-chain imino sugar *N*B-DGJ (Fig. 1B). Interestingly, HMA (400 µM) treatment enhanced both the initial rate of CF release from liposomes and likewise increased endpoint fluorescence compared to the DMSO control (Fig. 1C and D). In these assays Triton X-100 treatment yielded maximal fluorescence. This increase was likely due to either HMA induced fusion events, non-specific disruption of liposomes, or HMA holding the E5 channel complex in a more open conformation. In contrast addition of both *N*N-DNJ and *N*B-DGJ led to a significant reduction in 16E5-mediated CF release from liposomes, as measured by initial rate or endpoint fluorescence (Fig. 1E and F).

Next, FLAG-16E5 was pre-incubated with increasing concentrations of *N*N-DNJ (1–400 µM). *N*N-DNJ potently inhibited E5 viroporin activity in a dose-dependent fashion (Fig. 2A and B); plotting percentage initial rates were plotted against log10[*N*N-DNJ) (µM) and the approximate IC50 for *N*N-DNJ calculated to be 6.84 µM (Fig. 2C).

To confirm that imino sugars did not non-specifically block CF release from liposomes, the bee venom pore forming peptide Melittin was incubated with a high concentration (400 µM) of each imino sugar and the impact on CF release assessed by endpoint fluorescence. Compared to a Melittin only control neither imino sugar exerted any inhibitory effect on CF release (Fig. 2D). Finally, we confirmed that neither imino sugar could quench CF fluorescence intensities by incubating 400 µM compound with liposomes prior to disruption using Triton X-100 (0.5% w/v). As expected, none of the compounds displayed any ability to quench fluorescence (Fig. 2E), confirming that inhibition of FLAG-16E5 was protein-specific.

3.2. Molecular modelling of E5 – imino sugar interactions

To interrogate the potential mode of E5 inhibition by imino sugars we revisited our previous docking studies (Wetherill et al., 2012) and determined the probable binding modes of *N*N-DNJ and *N*B-DGJ using the Glide program (Schrodinger). Inhibitor compounds were docked into hexameric 16E5 models with the Glide grid extended to allow free docking of the each compound to the entire channel surface. Unlike previous studies where rimantadine occupied a lipophilic pocket in the lining of the channel lumen (Wetherill et al., 2012), *N*N-DNJ instead intercalated between E5 monomers at the protomer interface with a

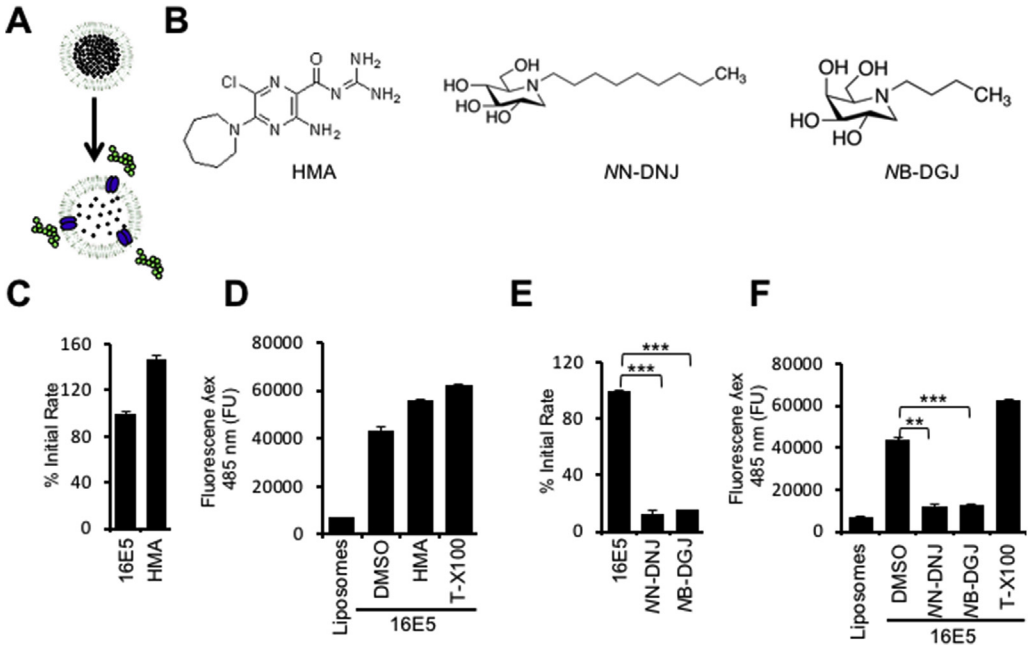

Fig. 1. HPV16 E5 viroporin activity is inhibited by imino sugars. (A) Schematic of the *in vitro* dye release assay. (B) Molecular structures of HMA, *N*N-DNJ and *N*B-DGJ. (C) The initial rate, calculated from the linear part of the real-time curve, for 16E5 plus DMSO represents 100%. The initial rate of CF release mediated by 16E5 in the presence of HMA was calculated as a percentage of the control initial rate. (D) Raw endpoint fluorescence measurements for CF release for liposomes alone, 16E5 and DMSO, 16E5 and HMA or Triton-X100. (E) Initial rates of CF release mediated by 16E5 in the presence of *N*N-DNJ or *N*B-DGJ. (F) Raw endpoint fluorescence measurements for CF liposomes mixed with 16E5, 16E5 and *N*N-DNJ, 16E5 and *N*B-DGJ or Triton X100. Error bars represent the standard deviation of the mean and one-way Anova analysis.

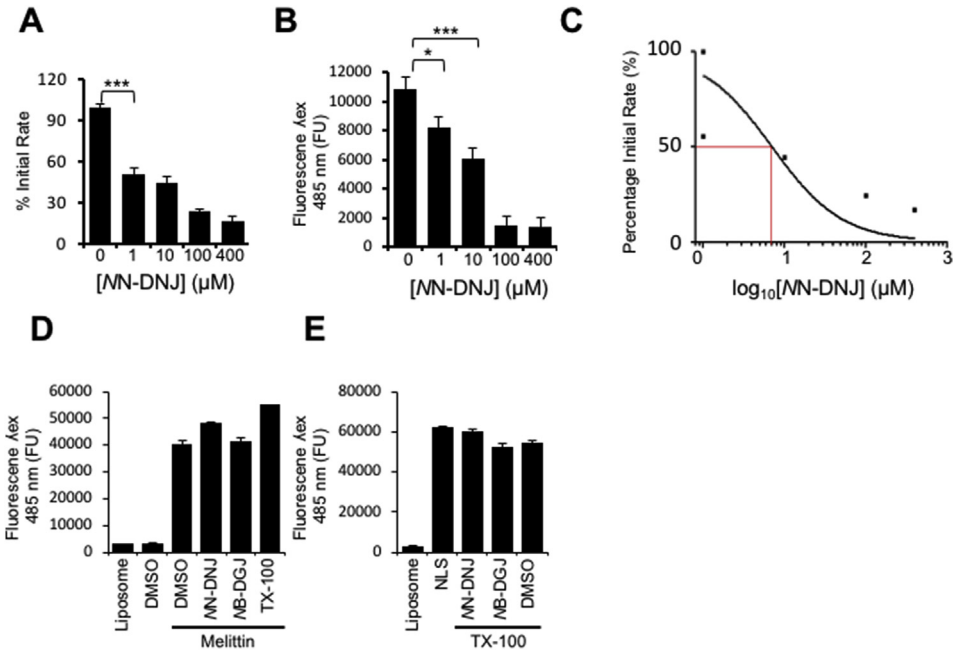

Fig. 2. Titratable effect of *N*N-DNJ on 16E5 mediated CF release. (A) CF liposomes were mixed with 16E5 which had been pre-incubated with varying concentrations of *N*N-DNJ. Initial rates of reactions were taken as a percentage of the initial rate generated by 16E5 in the absence of compound. (B) Endpoint fluorescence measurements for the above. (C) Percentage initial rates were plotted against the $\log_{10}$[*N*N-DNJ] and a regression curve was fitted. The x value at y + 50% was submitted into the formula IC50 = 10^X to calculate the approximate IC50 for *N*N-DNJ. (D) Imino sugars do not inhibit Melittin mediated dye release. Endpoint fluorescence measurements were recorded for liposomes mixed with Melittin in the presence of *N*N-DNJ, *N*B-DGJ or Triton-X100. (E) Endpoint fluorescence units for liposomes mixed with N-lauryl sarcosine (NLS) or Triton-X100 and imino sugars. Error bars represent the standard deviation of the mean and one-way Anova analysis was used to determine significance between selected samples.

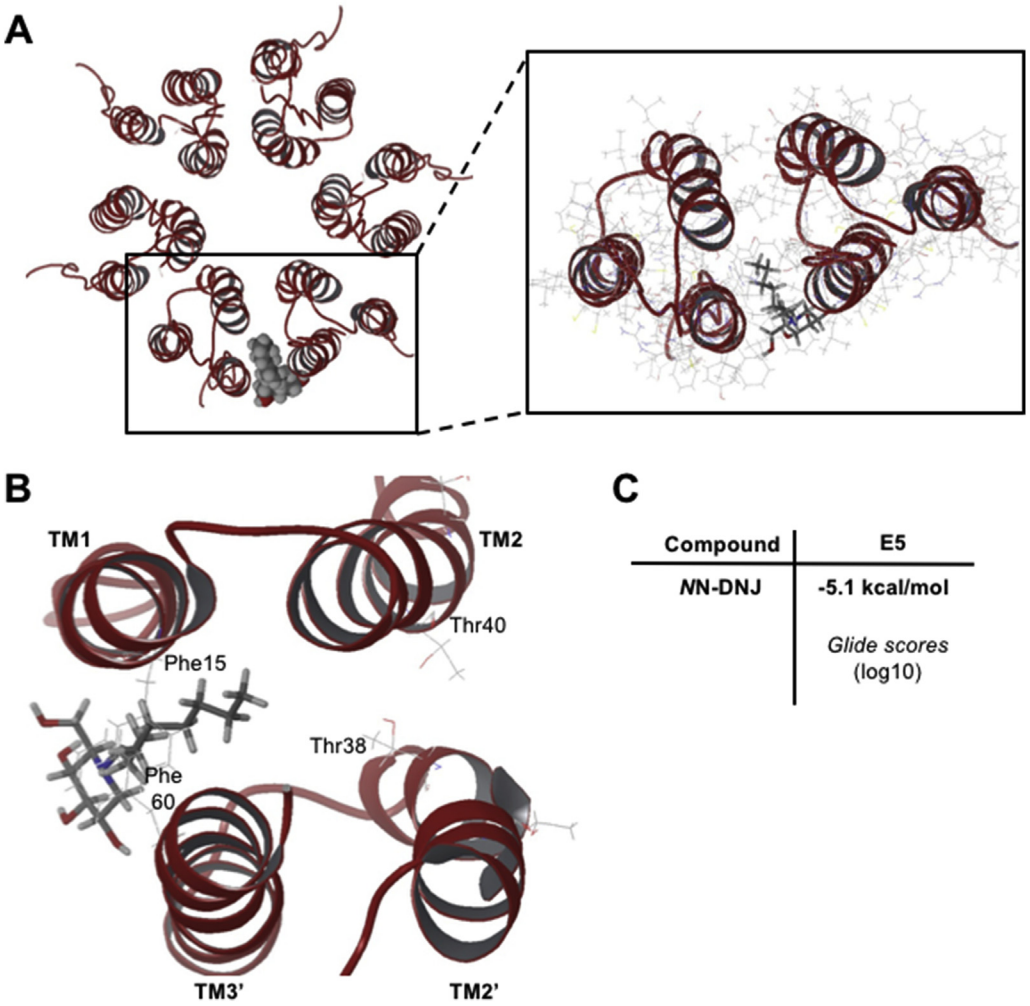

Fig. 3. Molecular modelling of 16E5 *N*N-DNJ interactions. (A) PyMol image of *N*N-DNJ preferentially docked between two adjacent 16E5 protomers within the channel complex. The secondary structure of 16E5 monomers were defined in ribbon format and the channel viewed from the C-terminus. *N*N-DNJ was depicted in sphere mode. (B) Magnified boxed region shows *N*N-DNJ (represented in stick format) partitioning between TM1 and TM3′ of two adjacent monomers. (C) Glidescore represents the predicted affinity of *N*N-DNJ (log10 kcal/mol) for the binding pocket depicted in (A).

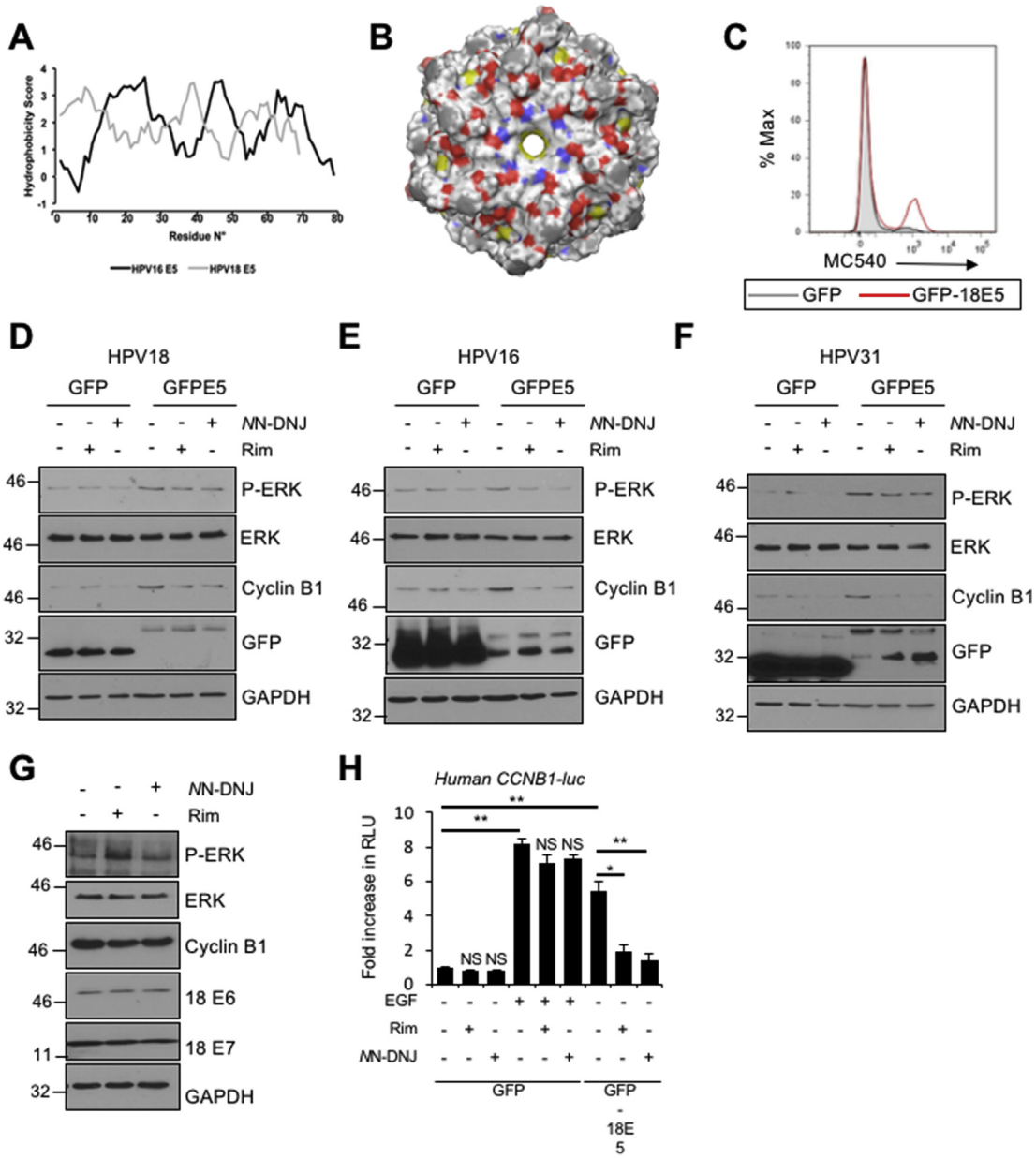

Fig. 4. Viroporin inhibitors prevent activation of MAPK signalling by E5 proteins. (A) Hydrophobicity plot of HPV16 and HPV18 E5 using the Kyte Doolittle programme. (B) Molecular modelling of full-length HPV18 E5 hexamer. Models of the E5 channel complex were generated by using Maestro as described in materials and methods. (C) Merocyanine assay performed on C33A cells transfected with GFP or GFP-18E5. Cells were analysed on BD Fortessa cytometer and histograms were created using FlowJo software. C33A cells were transfected with GFP-18E5 (D), GFP-16E5 (E) or GFP-31E5 (F) in parallel with a GFP control. Cells were then incubated with Rimantadine (100 μM) and *N*N-DNJ (100 μM) for 36 h and lysates probed with antibodies against cyclin B1, phosphorylated and total forms of ERK1/2 and GFP. GAPDH served as a loading control. Representative blots are shown from at least three independent biological repeats. (G) Lysates from HeLa cells incubated with Rimantadine (100 μM) and *N*N-DNJ (100 μM) for 48 h were probed with antibodies against the total and phosphorylated forms of ERK1/2, cyclin B1, HPV E6 and E7 oncoproteins and the loading control GAPDH. Representative blots are shown from at least three independent biological repeats. (H) HPV18 E5 activates a cyclin B1 reporter plasmid. C33A cells were co-transfected with the CCNB1 reporter and GFP or GFP-18E5 then subsequently treated with EGF, rimantadine or *N*N-DNJ, before cells were lysed in Passive Lysis Buffer (Promega) and analysed using a dual luciferase system (Promega). Data are from 3 independent biological repeats and presented as fold change compared to untreated GFP. Error bars are ± Standard deviation. *p < 0.05, **p < 0.01.

GlideScore of −5.1 kcal/mol (Fig. 3A). This was predicted to disrupt the pi stack generated by TM1 Phe15 and TM3' Phe60 (Fig. 3B), potentially disrupting oligomerisation of E5 protomers. *N*B-DGJ adopted a similar binding pose although was located closer to the pore, and also likely impairs the monomer interaction by disrupting the Thr38 – Thr40 hydrogen bond (Supplementary Fig. 1A). *N*B-DGJ had a similar estimated Glide docking score to *N*N-DNJ of −5.4 kcal/mol.

3.3. Viroporin inhibitors prevent activation of the ERK - cyclin B1 pathway by E5

We next wished to assess whether viroporin activity is a conserved feature of E5 proteins from other HPV types and ultimately to determine whether it contributes to the biological function of E5 in cells. Our laboratory has begun to study the functions of the E5 protein coded by HPV18 (Wasson et al., 2017). As such, we asked the question does 18E5, like 16E5, also possess viroporin activity? Despite relatively poor

amino acid conservation, the two proteins share similar hydrophobicity profiles indicating the presence of three TMD (Fig. 4A), and *in silico* modelling predicts the formation of an analogous 18E5 hexameric channel complex (Fig. 4B).

We were not able to purify recombinant 18E5 using our standard viroporin purification methods (Wetherill et al., 2012), and so were unable to undertake *in vitro* liposome assay studies with this protein. As an alternative strategy, we set out to examine potential 18E5 viroporin activity in cells. For this, we assessed the effect of 18E5 on membrane integrity using the lipophilic fluorescent dye Merocyanine 540 (MC540), which provides an indirect measure of lipid packing (Lelkes et al., 1980; Williamson et al., 1983) and has previously been used to investigate viroporin function (Suzuki et al., 2010). GFP-18E5/GFP transfected C33A cells were assessed for MC540 labelling using flow cytometry, which showed that the MC540 intensity in 18E5 cells was significantly higher than in GFP expressing cells (3 fold increase; $p = 0.01$) (Fig. 4C), suggesting that 18E5 disrupts lipid packing and modifies the structure of cellular membranes.

Consistent with previous observations, levels of ERK-MAPK phosphorylation, but not total protein, were increased in GFP-18E5 expressing cells compared to GFP alone and this correlated with an increase in cyclin B1 expression (Fig. 4D). This was reversed by addition of either rimantadine, *N*N-DNJ or *N*B-DGJ (Supplementary Fig. 1B) at 100 μM. This was not due to cytotoxic effects of these inhibitors (Supplementary Fig. 2). A similar reduction in ERK phosphorylation and cyclin B1 levels was observed in C33A cells expressing E5 proteins from high-risk HPV16 (Fig. 4E) and HPV31 (Fig. 4F) types treated with rimantadine or *N*N-DNJ yet compounds alone had no effect upon levels of basal ERK phosphorylation and cyclin B1 expression in GFP expressing cells (Fig. 4D–F and Supplementary Fig. 1B). Moreover, ERK phosphorylation and cyclin B1 expression were also unaltered in HeLa cells, which are HPV positive but lack E5, treated with Rimantadine or *N*N-DNJ (Fig. 4G).

Next, we assayed human cyclin B1 promoter driven transcription of firefly luciferase (CCNB1-luc) (Wasner et al., 2003) in cells co-transfected with this reporter and either GFP-18E5 or GFP. Luciferase activity was significantly higher in GFP-18E5 expressing C33A cells compared with GFP alone, and this was specifically reversed following treatment with either Rimantadine or *N*N-DNJ (Fig. 4H). Accordingly, neither rimantadine nor *N*N-DNJ affected luciferase activity in GFP-expressing C33A cells stimulated with EGF. Thus, E5 specific up-regulation of cyclin B1 expression following EGFR activation is sensitive to structurally unrelated prototypic viroporin inhibitors, which in turn display no off-target effects upon relevant pathways. Hence, we conclude that E5 viroporin activity is directly responsible for these effects.

3.4. Viroporin inhibitors prevent HPV18 E5 mediated mitogenic signalling in the context of productive HPV18 infection

Finally, we assessed the biological function of E5 viroporin activity in the context of the productive HPV life cycle. Primary human keratinocytes harbouring the wild-type (WT) or an E5KO HPV18 genome were differentiated in high calcium media in the presence/absence of 50 μM Rimantadine (Fig. 5A), *N*N-DNJ (Fig. 5B) or *N*B-DGJ (Supplementary Fig. 1C). Again, inhibitors were able to reverse the retention of ERK phosphorylation and cyclin B1 expression in the presence of differentiation stimuli, reducing them to similar levels observed in cells harbouring the E5KO genome (compare lanes 2 and 3 plus 3 and 5). As a consequence of the loss of mitogenic signalling we noted that wild type cells treated with viroporin inhibitors exhibited an increase in differentiation marker expression. Thus, taken together our data demonstrate that E5 viroporin activity is critical for maintenance of mitogenic signalling and the delay in differentiation marker expression observed during the productive stages of the HPV18 life cycle.

4. Discussion

This work provides evidence linking the viroporin activity of high risk HPV E5 proteins (types 16, 18 and 31) with a critical aspect of their function within cells. We also show that alkylated imino-sugars represent a second class of prototypic viroporin inhibitor compounds which, in addition to the previously identified E5 blocker, rimantadine, prevent E5-mediated upregulation of cyclin B1 expression via its effects upon EGFR activation. Hence, E5 represents the first example of a potentially oncogenic viroporin, making it an excellent prospective target for both antiviral and stratified anti-tumour strategies.

Treatment with both long and short chain alkyl-chain imino sugar derivatives reduced HPV16 E5 viroporin activity *in vitro*. In particular, *N*N-DNJ exhibited considerable *in vitro* potency ($[IC_{50}] \sim 6.84$ μM), representing an improvement compared with previous studies of rimantadine or bespoke scaffolds including MV006 (Wetherill et al., 2012). However, the potency of both compounds appeared similar in cell-based assays in the low-mid micromolar range. This is reminiscent of activity vs. other viroporins for which such prototypic molecules are shown to have activity, including e.g. hepatitis C virus p7 and IAV M2.

However, whilst lacking true drug-like potency, prototypic viroporin inhibitors are useful for identifying both potential binding sites and inhibitory modes of action that can subsequently be targeted via rational design or compound screening approaches. Unlike rimantadine, *N*N-DNJ is predicted to intercalate between protomers within validated molecular models of the HPV16 E5 channel complex, suggesting that interrupting oligomerisation represents a potential inhibitory mechanism for these compounds. Specifically, *N*N-DNJ binding to the 16E5 channel is predicted to disrupt the pi stack generated by TM1 Phe15 and TM3' Phe60, reducing the stability of protomer-protomer binding. Interestingly, alignment of E5 amino acid sequence identifies equivalent Phe residues in the mucosal HPV types, suggesting that if these residues do mediate oligomerisation then *N*N-DNJ may have the potential for cross-activity against several HPV types. Similarly, *N*N-DNJ was shown to prevent HCV p7 oligomerisation, with a similar inter-protomer binding site predicted by docking studies (Foster et al., 2011). This binding site was validated by the co-location of a resistance polymorphism, F25A, within the site, identified through the innate *N*N-DNJ resistance of genotype 3a p7. As we have employed a similar modelling/docking strategy herein, this highlights a potential mechanistic similarity between 16E5 and p7 oligomerisation, which should be further investigated. Lastly, it is notable that shorter chain imino sugars (e.g. *N*B-DGJ) could inhibit 16E5 viroporin activity *in vitro*. These compounds are ineffective against other viroporins, including p7 (Steinmann et al., 2007). Analysis of the *N*B-DGJ binding mode suggested that it also interacts with E5 at the protomer interface which would likely interfere with channel oligomerisation. Satisfied that both rimantadine and the imino sugars represented inhibitors of E5 channel function, we employed them as tools with which to dissect the potential link between E5 viroporin activity and key aspects of E5 function within cells.

The role of E5 in HPV-associated cancers remains poorly defined. As HPV genomes often become integrated during malignant progression, disrupting the E5 ORF, it has been assumed that E5 might play a cancer-promoting role rather than driving progression or persistence post-transformation. However, a significant number (~15%) of cervical cancers contain unintegrated HPV genomes and a much lower frequency of viral DNA integration occurs in HPV positive HNSCC (Morgan et al., 2017; Olthof et al., 2014). Moreover, E5 protein can be detected by mass spectrometry in cervical cancer cell lines containing an integrated HPV genome (Sahab et al., 2012). Therefore, E5 expression likely persists within a subset of advanced HPV positive tumours. This could expedite stratification of therapy for such patients, consistent with the growing recognition that E5 constitutes a potential therapeutic target (Kim and Yang, 2006; Maufort et al., 2010b).

A major aspect of E5 oncogenic function is the activation of EGFR

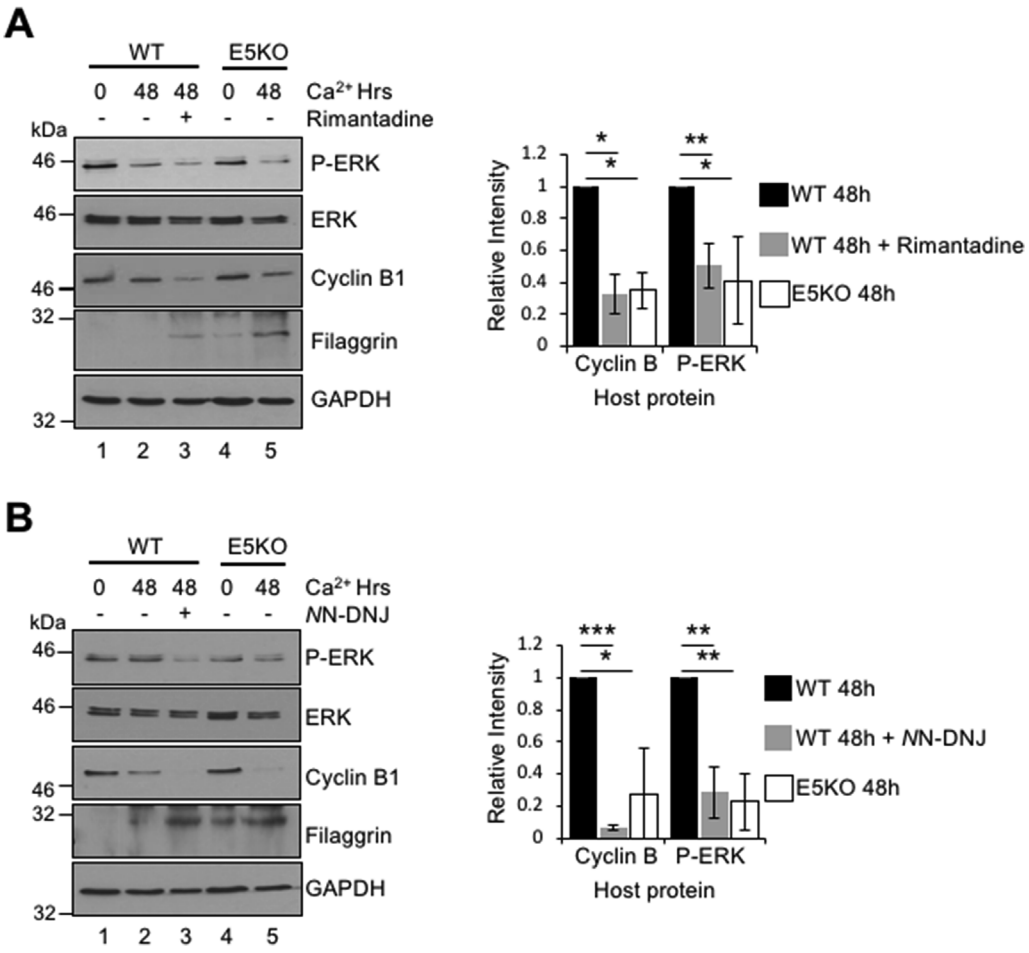

Fig. 5. Viroporin inhibitors prevent HPV18 E5 mediated mitogenic signalling in the context of productive HPV18 infection. Primary human keratinocytes containing wild type or E5KO HPV18 genomes were differentiated in high calcium media for 48 h in the presence of absence of (A) rimantadine (50 μM) and (B) *N*N-DNJ (50 μM) and cell lysates probed with antibodies against cyclin B1, the phosphorylated and total forms of ERK1/2, Filaggrin and the GAPDH loading control. Representative blots are shown from at least three independent biological repeats. Graphs represent densitometry analysis of cyclin B1 and phosphorylated ERK levels at the 48 h time point for untreated and drug-treated wild type and the E5KO cells. Graphs represent data from three independent repeats. *p < 0.05, **p < 0.01, ***p < 0.001.

signalling to drive cyclin B1 expression via ERK in the suprabasal layers of the epithelium (Wasson et al., 2017). Interestingly, this likely involves alkalinisation of EGFR-containing endosomes; this was originally ascribed to interactions between E5 and cellular vATPase (Conrad et al., 1993), yet this is now thought not to be the case (Suprynowicz et al., 2010). Our previous observation that acidic pH activates E5 channel activity *in vitro* is reminiscent of other viroporins such as p7 and M2, both of which serve to promote vesicle alkalinisation. Consistent with a similar role for high risk E5 in cells, treatment of E5 expressing keratinocytes, or cells harbouring full-length HPV genomes, with rimantadine or imino sugars prevented increased cyclin B expression and concomitant ERK phosphorylation. Inhibitors had no obvious off-target effects, with neither cells expressing GFP alone, nor HPV-transformed cell lines with integrated genomes lacking E5, showing any modulation of the pathway upon treatment. This observation was consistent between E5 from three high-risk HPV types, suggesting that the link between E5 viroporin activity and at least one major aspect of its pro-oncogenic function are directly linked.

Taken together, our data supports that E5 is unique amongst viroporins as the only example known to date where channel activity has a direct role regulating cellular proliferation and potentially also malignant transformation. Identification of prototypic inhibitors suggests that druggable sites exist within the E5 channel complex that could be exploited by dedicated small molecule drug discovery programmes. This could lead to new therapeutic options stratified for patients with tumours that maintain E5 expression, or indeed as an antiviral strategy for HPV positive individuals prior to the onset of malignancy.

5. Conclusion

Prototypic viroporin inhibitors from distinct chemotypes are effective inhibitors of E5 viroporin activity *in vitro* and in primary cell culture models, abolishing ERK-MAPK activation and reducing cyclin B1 expression. The distinct mode of action of adamantanes versus imino sugars provides scope for the development of parallel yet complementary E5 inhibitor series that could comprise combination therapies. These could be utilised for stratified treatment of HPV associated tumours prior to virus integration, or as true antiviral therapies to eliminate virus prior to malignant transformation.

Conflicts of interest

The authors declare that there is no conflict of interest.

Financial statement

The work was funded by grants to AM from Cancer Research UK (C43832/A14246 and C37059/A11941), the Medical Research Council (MRC) (MR/K012665/1), a Biotechnology and Biological Sciences Research Council (BBSRC) studentship (DK BB/M011151/1) and a Wellcome Trust studentship (GS 109157/Z/15/Z). The funders had no role in study design, data collection and analysis, decision to publish, or preparation of the manuscript.

Acknowledgements

We thank Kurt Engeland (University of Leipzig) for providing human CCNB1 luciferase reporter plasmids and Joseph Spitzer and his

patients for the collection and donation of foreskin tissue.

Appendix A. Supplementary data

Supplementary data related to this article can be found at https://doi.org/10.1016/j.antiviral.2018.08.005.

References

Bruni, L., Diaz, M., Barrionuevo-Rosas, L., Herrero, R., Bray, F., Bosch, F.X., de Sanjose, S., Castellsagué, X., 2016. Global estimates of human papillomavirus vaccination coverage by region and income level: a pooled analysis. Lancet Glob. Health 4, e453–e463. https://doi.org/10.1016/S2214-109X(16)30099-7.

Cates, W., 1999. Estimates of the incidence and prevalence of sexually transmitted diseases in the United States. American Social Health Association Panel. Sex. Transm. Dis. 26, S2–S7.

Chang, J.L., Tsao, Y.P., Liu, D.W., Huang, S.J., Lee, W.H., Chen, S.-L., 2001. The expression of HPV-16 E5 protein in squamous neoplastic changes in the uterine cervix. J. Biomed. Sci. 8, 206–213.

Conrad, M., Bubb, V.J., Schlegel, R., 1993. The human papillomavirus type 6 and 16 E5 proteins are membrane-associated proteins which associate with the 16-kilodalton pore-forming protein. J. Virol. 67, 6170–6178.

de Sanjose, S., Quint, W.G., Alemany, L., Geraets, D.T., Klaustermeier, J.E., Lloveras, B., Tous, S., Felix, A., Bravo, L.E., Shin, H.-R., Vallejos, C.S., de Ruiz, P.A., Lima, M.A., Guimera, N., Clavero, O., Alejo, M., Llombart-Bosch, A., Cheng-Yang, C., Tatti, S.A., Kasamatsu, E., Iljazovic, E., Odida, M., Prado, R., Seoud, M., Grce, M., Usubutun, A., Jain, A., Suarez, G.A.H., Lombardi, L.E., Banjo, A., Menéndez, C., Domingo, E.J., Velasco, J., Nessa, A., Chichareon, S.C.B., Qiao, Y.L., Lerma, E., Garland, S.M., Sasagawa, T., Ferrera, A., Hammouda, D., Mariani, L., Pelayo, A., Steiner, I., Oliva, E., Meijer, C.J., Al-Jassar, W.F., Cruz, E., Wright, T.C., Puras, A., Llave, C.L., Tzardi, M., Agorastos, T., Garcia-Barriola, V., Clavel, C., Ordi, J., Andújar, M., Castellsagué, X., Sánchez, G.I., Nowakowski, A.M., Bornstein, J., Muñoz, N., Bosch, F.X., Retrospective International Survey and HPV Time Trends Study Group, 2010. Human papillomavirus genotype attribution in invasive cervical cancer: a retrospective cross-sectional worldwide study. Lancet Oncol. 11, 1048–1056. https://doi.org/10.1016/S1470-2045(10)70230-8.

Delury, C.P., Marsh, E.K., James, C.D., Boon, S.S., Banks, L., Knight, G.L., Roberts, S., 2013. The role of protein kinase A regulation of the E6 PDZ-binding domain during the differentiation-dependent life cycle of human papillomavirus type 18. J. Virol. 87, 9463–9472. https://doi.org/10.1128/JVI.01234-13.

Eldridge, M.D., Murray, C.W., Auton, T.R., Paolini, G.V., Mee, R.P., 1997. Empirical scoring functions: I. The development of a fast empirical scoring function to estimate the binding affinity of ligands in receptor complexes. J. Comput. Aided Mol. Des. 11, 425–445.

Fehrmann, F., Klumpp, D.J., Laimins, L.A., 2003. Human papillomavirus type 31 E5 protein supports cell cycle progression and activates late viral functions upon epithelial differentiation. J. Virol. 77, 2819–2831.

Foster, T.L., Verow, M., Wozniak, A.L., Bentham, M.J., Thompson, J., Atkins, E., Weinman, S.A., Fishwick, C., Foster, R., Harris, M., Griffin, S., 2011. Resistance mutations define specific antiviral effects for inhibitors of the hepatitis C virus p7 ion channel. Hepatology 54, 79–90. https://doi.org/10.1002/hep.24371.

Friesner, R.A., Banks, J.L., Murphy, R.B., Halgren, T.A., Klicic, J.J., Mainz, D.T., Repasky, M.P., Knoll, E.H., Shelley, M., Perry, J.K., Shaw, D.E., Francis, P., Shenkin, P.S., 2004. Glide: a new approach for rapid, accurate docking and scoring. 1. Method and assessment of docking accuracy. J. Med. Chem. 47, 1739–1749. https://doi.org/10.1021/jm0306430.

Genther Williams, S.M., Disbrow, G.L., Schlegel, R., Lee, D., Threadgill, D.W., Lambert, P.F., 2005. Requirement of epidermal growth factor receptor for hyperplasia induced by E5, a high-risk human papillomavirus oncogene. Canc. Res. 65, 6534–6542. https://doi.org/10.1158/0008-5472.CAN-05-0083.

Genther, S.M., Sterling, S., Duensing, S., Münger, K., Sattler, C., Lambert, P.F., 2003. Quantitative role of the human papillomavirus type 16 E5 gene during the productive stage of the viral life cycle. J. Virol. 77, 2832–2842.

Kim, S.-W., Yang, J.-S., 2006. Human papillomavirus type 16 E5 protein as a therapeutic target. Yonsei Med. J. 47, 1–14. https://doi.org/10.3349/ymj.2006.47.1.1.

Lelkes, P.I., Bach, D., Miller, I.R., 1980. Perturbations of membrane structure by optical probes: II. Differential scanning calorimetry of dipalmitoyllecithin and its analogs interacting with Merocyanine 540. J. Membr. Biol. 54, 141–148.

Mankouri, J., Fragkoudis, R., Richards, K.H., Wetherill, L.F., Harris, M., Kohl, A., Elliott, R.M., Macdonald, A., 2010. Optineurin negatively regulates the induction of IFNβ in response to RNA virus infection. PLoS Pathog. 6, e1000778. https://doi.org/10.1371/journal.ppat.1000778.

Maufort, J.P., Shai, A., Pitot, H.C., Lambert, P.F., 2010a. A role for HPV16 E5 in cervical carcinogenesis. Canc. Res. 70, 2924–2931. https://doi.org/10.1158/0008-5472.CAN-09-3436.

Maufort, J.P., Shai, A., Pitot, H.C., Lambert, P.F., 2010b. A role for HPV16 E5 in cervical carcinogenesis. Canc. Res. 70, 2924–2931. https://doi.org/10.1158/0008-5472.CAN-09-3436.

Maufort, J.P., Williams, S.M.G., Pitot, H.C., Lambert, P.F., 2007. Human papillomavirus 16 E5 oncogene contributes to two stages of skin carcinogenesis. Canc. Res. 67, 6106–6112. https://doi.org/10.1158/0008-5472.CAN-07-0921.

Moody, C.A., Laimins, L.A., 2010. Human papillomavirus oncoproteins: pathways to transformation. Nat. Rev. Cancer 10, 550–560. https://doi.org/10.1038/nrc2886.

Morgan, I.M., DiNardo, L.J., Windle, B., 2017. Integration of human papillomavirus genomes in head and neck cancer: is it time to consider a paradigm shift? Viruses 9, 208. https://doi.org/10.3390/v9080208.

Müller, Marietta, Prescott, E.L., Wasson, C.W., Macdonald, A., 2015a. Human Papillomavirus E5 Oncoprotein: Function and Potential Target for Antiviral Therapeutics. https://doi.org/10.2217/fvl.14.99 10, 27–39. doi:10.2217/fvl.14.99.

Müller, Marietta, Wasson, C.W., Bhatia, R., Boxall, S., Millan, D., Goh, G.Y.S., Haas, J., Stonehouse, N.J., Macdonald, A., 2015b. YIP1 family member 4 (YIPF4) is a novel cellular binding partner of the papillomavirus E5 proteins. Sci. Rep. 5, 12523. https://doi.org/10.1038/srep12523.

Olthof, N.C., Speel, E.-J.M., Kolligs, J., Haesevoets, A., Henfling, M., Ramaekers, F.C.S., Preuss, S.F., Drebber, U., Wieland, U., Silling, S., Lam, W.L., Vucic, E.A., Kremer, B., Klussmann, J.-P., Huebbers, C.U., 2014. Comprehensive analysis of HPV16 integration in OSCC reveals no significant impact of physical status on viral oncogene and virally disrupted human gene expression. PLoS One 9, e88718. https://doi.org/10.1371/journal.pone.0088718.

Pavlović, D., Neville, D.C.A., Argaud, O., Blumberg, B., Dwek, R.A., Fischer, W.B., Zitzmann, N., 2003. The hepatitis C virus p7 protein forms an ion channel that is inhibited by long-alkyl-chain iminosugar derivatives. Proc. Natl. Acad. Sci. U.S.A. 100, 6104–6108. https://doi.org/10.1073/pnas.1031527100.

Pinto, L.H., Holsinger, L.J., Lamb, R.A., 1992. Influenza virus M2 protein has ion channel activity. Cell 69, 517–528.

Prigge, E.S., Knebel Doeberitz von, M., Reuschenbach, M., 2017. Clinical relevance and implications of HPV-induced neoplasia in different anatomical locations. Mutat. Res. Rev. Mutat. Res. 772, 51–66. https://doi.org/10.1016/j.mrrev.2016.06.005.

Richards, K.H., Wasson, C.W., Watherston, O., Doble, R., Blair, G.E., Wittmann, M., Macdonald, A., 2015. The human papillomavirus (HPV) E7 protein antagonises an Imiquimod-induced inflammatory pathway in primary human keratinocytes. Sci. Rep. 5, 12922. https://doi.org/10.1038/srep12922.

Royle, J., Dobson, S.J., Müller, M., Macdonald, A., 2015. Emerging roles of viroporins encoded by DNA viruses: novel targets for antivirals? Viruses 7, 5375–5387. https://doi.org/10.3390/v7102880.

Sahab, Z., Sudarshan, S.R., Liu, X., Zhang, Y., Kirilyuk, A., Kamonjoh, C.M., Simic, V., Dai, Y., Byers, S.W., Doorbar, J., Suprynowicz, F.A., Schlegel, R., 2012. Quantitative measurement of human papillomavirus type 16 e5 oncoprotein levels in epithelial cell lines by mass spectrometry. J. Virol. 86, 9465–9473. https://doi.org/10.1128/JVI.01032-12.

Samson, A., Bentham, M.J., Scott, K., Nuovo, G., Bloy, A., Appleton, E., Adair, R.A., Dave, R., Peckham-Cooper, A., Toogood, G., Nagamori, S., Coffey, M., Vile, R., Harrington, K., Selby, P., Errington-Mais, F., Melcher, A., Griffin, S., 2016. Oncolytic reovirus as a combined antiviral and anti-tumour agent for the treatment of liver cancer. Gut gutjnl 2016, 312009. https://doi.org/10.1136/gutjnl-2016-312009.

Schiller, J.T., Müller, Martin, 2015. Next generation prophylactic human papillomavirus vaccines. Lancet Oncol. 16, e217–e225. https://doi.org/10.1016/S1470-2045(14)71179-9.

Scott, C., Griffin, S.D.C., 2015. Viroporins: structure, function and potential as antiviral targets. J. Gen. Virol. https://doi.org/10.1099/vir.0.000201.

Steinmann, E., Whitfield, T., Kallis, S., Dwek, R.A., Zitzmann, N., Pietschmann, T., Bartenschlager, R., 2007. Antiviral effects of amantadine and iminosugar derivatives against hepatitis C virus. Hepatology 46, 330–338. https://doi.org/10.1002/hep.21686.

Stgelais, C., Foster, T.L., Verow, M., Atkins, E., Fishwick, C.W.G., Rowlands, D., Harris, M., Griffin, S., 2009. Determinants of hepatitis C virus p7 ion channel function and drug sensitivity identified in vitro. J. Virol. 83, 7970–7981. https://doi.org/10.1128/JVI.00521-09.

Stoler, M.H., Rhodes, C.R., Whitbeck, A., Wolinsky, S.M., Chow, L.T., Broker, T.R., 1992. Human papillomavirus type 16 and 18 gene expression in cervical neoplasias. Hum. Pathol. 23, 117–128.

Straight, S.W., Herman, B., McCance, D.J., 1995. The E5 oncoprotein of human papillomavirus type 16 inhibits the acidification of endosomes in human keratinocytes. J. Virol. 69, 3185–3192.

Straight, S.W., Hinkle, P.M., Jewers, R.J., McCance, D.J., 1993. The E5 oncoprotein of human papillomavirus type 16 transforms fibroblasts and effects the downregulation of the epidermal growth factor receptor in keratinocytes. J. Virol. 67, 4521–4532.

Suprynowicz, F.A., Krawczyk, E., Hebert, J.D., Sudarshan, S.R., Simic, V., Kamonjoh, C.M., Schlegel, R., 2010. The human papillomavirus type 16 E5 oncoprotein inhibits epidermal growth factor trafficking independently of endosome acidification. J. Virol. 84, 10619–10629. https://doi.org/10.1128/JVI.00831-10.

Suzuki, T., Orba, Y., Okada, Y., Sunden, Y., Kimura, T., Tanaka, S., Nagashima, K., Hall, W.W., Sawa, H., 2010. The human polyoma JC virus agnoprotein acts as a viroporin. PLoS Pathog. 6, e1000801. https://doi.org/10.1371/journal.ppat.1000801.

Walboomers, J.M., Jacobs, M.V., Manos, M.M., Bosch, F.X., Kummer, J.A., Shah, K.V., Snijders, P.J., Peto, J., Meijer, C.J., Muñoz, N., 1999. Human papillomavirus is a necessary cause of invasive cervical cancer worldwide. J. Pathol. 189, 12–19. https://doi.org/10.1002/(SICI)1096-9896(199909)189:1<12::AID-PATH431>3.0.CO;2-F.

Wasner, M., Tschöp, K., Spiesbach, K., Haugwitz, U., Johne, C., Mössner, J., Mantovani, R., Engeland, K., 2003. Cyclin B1 transcription is enhanced by the p300 coactivator and regulated during the cell cycle by a CHR-dependent repression mechanism. FEBS Lett. 536, 66–70.

Wasson, C.W., Morgan, E.L., Müller, M., Ross, R.L., Hartley, M., Roberts, S., Macdonald, A., 2017. Human papillomavirus type 18 E5 oncogene supports cell cycle progression and impairs epithelial differentiation by modulating growth factor receptor signalling during the virus life cycle. Oncotarget 8, 103581–103600. https://doi.org/10.18632/oncotarget.21658.

Wetherill, L.F., Holmes, K.K., Verow, M., Müller, M., Howell, G., Harris, M., Fishwick, C., Stonehouse, N., Foster, R., Blair, G.E., Griffin, S., Macdonald, A., 2012. High-risk

human papillomavirus E5 oncoprotein displays channel-forming activity sensitive to small-molecule inhibitors. J. Virol. 86, 5341–5351. https://doi.org/10.1128/JVI.06243-11.

Williamson, P., Mattocks, K., Schlegel, R.A., 1983. Merocyanine 540, a fluorescent probe sensitive to lipid packing. Biochim. Biophys. Acta 732, 387–393.

Wilson, L., Gage, P., Ewart, G., 2006. Hexamethylene amiloride blocks E protein ion channels and inhibits coronavirus replication. Virology 353, 294–306. https://doi.org/10.1016/j.virol.2006.05.028.

Wilson, R., Fehrmann, F., Laimins, L.A., 2005. Role of the E1–E4 protein in the differentiation-dependent life cycle of human papillomavirus type 31. J. Virol. 79, 6732–6740. https://doi.org/10.1128/JVI.79.11.6732-6740.2005.

Wu, S.-F., Lee, C.-J., Liao, C.-L., Dwek, R.A., Zitzmann, N., Lin, Y.-L., 2002. Antiviral effects of an iminosugar derivative on flavivirus infections. J. Virol. 76, 3596–3604. https://doi.org/10.1128/JVI.76.8.3596-3604.2002.

Zitzmann, N., Mehta, A.S., Carrouée, S., Butters, T.D., Platt, F.M., McCauley, J., Blumberg, B.S., Dwek, R.A., Block, T.M., 1999. Imino sugars inhibit the formation and secretion of bovine viral diarrhea virus, a pestivirus model of hepatitis C virus: implications for the development of broad spectrum anti-hepatitis virus agents. Proc. Natl. Acad. Sci. U.S.A. 96, 11878–11882.